

# Lens models of galaxy–galaxy strong lenses

BDLensing team<sup>1</sup> and C. Ptolemy<sup>2,\*</sup>

<sup>1</sup> Institute for Astronomy (IfA), University of Vienna, Türkenschanzstrasse 17, A-1180 Vienna  
e-mail: wuchterl@amok.ast.univie.ac.at

<sup>2</sup> University of Alexandria, Department of Geography, ...  
e-mail: c.ptolemy@hipparch.uheaven.space \*\*

Received September 15, 1996; accepted March 16, 1997

## ABSTRACT

**Context.** To investigate the physical nature of the ‘nucleated instability’ of proto giant planets, the stability of layers in static, radiative gas spheres is analysed on the basis of Baker’s standard one-zone model.

**Aims.** It is shown that stability depends only upon the equations of state, the opacities and the local thermodynamic state in the layer. Stability and instability can therefore be expressed in the form of stability equations of state which are universal for a given composition.

**Methods.** The stability equations of state are calculated for solar composition and are displayed in the domain  $-14 \leq \lg \rho / [\text{g cm}^{-3}] \leq 0$ ,  $8.8 \leq \lg e / [\text{erg g}^{-1}] \leq 17.7$ . These displays may be used to determine the one-zone stability of layers in stellar or planetary structure models by directly reading off the value of the stability equations for the thermodynamic state of these layers, specified by state quantities as density  $\rho$ , temperature  $T$  or specific internal energy  $e$ . Regions of instability in the  $(\rho, e)$ -plane are described and related to the underlying microphysical processes.

**Results.** Vibrational instability is found to be a common phenomenon at temperatures lower than the second He ionisation zone. The  $\kappa$ -mechanism is widespread under ‘cool’ conditions.

**Key words.** giant planet formation –  $\kappa$ -mechanism – stability of gas spheres

## 1. Introduction

Strong gravitational lensing is the phenomenon of forming multiple images from a background source due to the gravitational bending of light path by a massive foreground deflector, such as a galaxy, galaxy group, or cluster. As a result, strong lensing systems are powerful probes of the mass distribution of the foreground deflector (see [Shajib et al. 2022](#), for a review on strong lensing by galaxies).

Whereas the observed light traces the stars in a lensing galaxy, strong lensing traces the total matter distribution, including dark and baryonic components. As a result, strong lensing can be used to study the relative alignment between dark matter and stars. Any detected offset between these two components can indicate self-interaction in the dark matter particles ([Harvey et al. 2014](#); [Kahlhoefer et al. 2014](#); [Robertson et al. 2017](#)). In the  $\Lambda$  cold dark matter ( $\Lambda$ CDM) cosmology – the current paradigm to describe our Universe – the EAGLE simulation predicts no significant offset  $\sim 200$  pc, regardless of the galaxy being a field galaxy or a cluster member ([Schaller et al. 2015](#)). Although a recent merger can lead to an offset between the dark matter and stars, these systems are statistically very rare ([Schaller et al. 2015](#)). On the observational front, only one system has been observed with an offset much larger than this prediction ( $1.72 \pm 0.42$  kpc), where the deflector consists of two merging galaxies ([Shu et al. 2016](#)). [Shajib et al. \(2019\)](#) find a root-mean-square (RMS) offset in a sample of 13 strong lenses to be  $0''.04$  (i.e.,  $\sim 200$  pc at  $z \sim 0.5$ ) excluding three outliers, one of which has two comparable-mass deflectors potentially residing in the

same parent halo. Similarly, [Shajib et al. \(2021\)](#) constrained a 68 percent upper limit of  $218 \pm 19$  pc from a sample of 23 galaxy–galaxy lenses.

The misalignment between the mass and light distributions can also be traced using the position angles of the major axes of the elliptical galaxies, which are the most common type of deflectors at the galaxy scale. Previous studies mostly found tight alignment within  $\sim 10^\circ$  ([Keeton et al. 1998](#); [Kochanek 2002](#); [Treu et al. 2009](#); [Gavazzi et al. 2012](#); [Sluse et al. 2012](#); [Bruderer et al. 2016](#); [Shajib et al. 2019, 2021](#)), with higher misalignments are accompanied by large “external” shear magnitude, although the vice versa is not necessary. The accompaniment of a large “external” shear with a large misalignment can be interpreted as systems in a crowded environment that are not yet dynamically relaxed, as they can have stellar orbits misaligned with the underlying dark matter distribution. Simulations found highly misaligned orbits in isolated systems to be unstable and rare ([Heiligman & Schwarzschild 1979](#); [Martinet & de Zeeuw 1988](#); [Adams et al. 2007](#); [Debattista et al. 2015](#)). However, this interpretation treats “external” shear as originating purely from nearby line-of-sight galaxies external to the central deflector. Interestingly, [Etherington et al. \(2023\)](#) suggested that this “external” shear is not purely of external origin and can arise from the inadequacy of the mass model for lensing galaxy in capturing all of its angular complexity (for example, boxy/discyness, ellipticity gradient, isophotal twists; [Van de Vyvere et al. 2022a,b](#)). This suggestion from [Etherington et al. \(2023\)](#) makes the explanation of high misalignment as stemming from interaction with a crowded environment less favorable.

In this paper, we investigate the alignment between the mass and light using a sample of 20 galaxies. We present power-law

\* Just to show the usage of the elements in the author field

\*\* The university of heaven temporarily does not accept e-mails

mass models of these systems based on *Hubble Space Telescope* (*HST*) imaging data. Using our lens models, we perform two experiments. First, we check if there is a difference in the mass and light offset between isolated and non-isolated galaxies and test the prediction of no difference from the EAGLE simulation. Second, we investigate if the misalignment between light and mass major axes directly correlates with the local galaxy density. This second experiment more directly tests the hypothesis that galaxies with stellar orbits misaligned with dark matter live in crowded environments without adopting the “external” shear as a measure of a crowded environment.

This paper is organized as follows. In Section 2, we describe our lens sample and the *HST* data we model. Then in Section 3, we describe our lens modelling method. We present our results in Section 4. Finally, we discuss our result and conclude the paper in Section 5. Throughout the paper, we adopt a flat  $\Lambda$ CDM cosmology as the fiducial cosmology with  $H_0 = 70 \text{ km s}^{-1} \text{ Mpc}^{-1}$  and  $\Omega_m = 0.3$ .

## 2. Data

### 2.1. *HST* imaging

### 2.2. Description of special systems (can be finalized later)

## 3. Lens modelling (Method)

### 3.1. Lens model ingredients

#### 3.1.1. Mass profile

#### 3.1.2. Light profiles

### 3.2. Modelling procedure

## 4. Result

### 4.1. Lens model parameters

### 4.2. Estimation of $\Sigma_{10}$

### 4.3. Mass and light alignment

## 5. Discussion and conclusion

*Acknowledgements.* Part of this work was supported by the German *Deutsche Forschungsgemeinschaft*, DFG project number Ts 17/2–1.

## References

- Adams, F. C., Bloch, A. M., Butler, S. C., Druce, J. M., & Ketchum, J. A. 2007, *ApJ*, 670, 1027
- Bruderer, C., Read, J. I., Coles, J. P., et al. 2016, *MNRAS*, 456, 870
- Debattista, V. P., van den Bosch, F. C., Roškar, R., et al. 2015, *MNRAS*, 452, 4094
- Etherington, A., Nightingale, J. W., Massey, R., et al. 2023, Strong gravitational lensing’s ‘external shear’ is not shear
- Gavazzi, R., Treu, T., Marshall, P. J., Brault, F., & Ruff, A. 2012, *ApJ*, 761, 170
- Harvey, D., Tittley, E., Massey, R., et al. 2014, *Monthly Notices of the Royal Astronomical Society*, 441, 404
- Heiligman, G. & Schwarzschild, M. 1979, *ApJ*, 233, 872
- Kahlhoefer, F., Schmidt-Hoberg, K., Frandsen, M. T., & Sarkar, S. 2014, *Monthly Notices of the Royal Astronomical Society*, 437, 2865
- Keeton, C. R., Kochanek, C. S., & Falco, E. E. 1998, *ApJ*, 509, 561
- Kochanek, C. S. 2002, in *The Shapes of Galaxies and their Dark Halos*, ed. P. Natarajan (WORLD SCIENTIFIC), 62–71
- Martinet, L. & de Zeeuw, T. 1988, *A&A*, 206, 269
- Robertson, A., Massey, R., & Eke, V. 2017, *Monthly Notices of the Royal Astronomical Society*, 467, 4719
- Schaller, M., Frenk, C. S., Bower, R. G., et al. 2015, *MNRAS*, 452, 343
- Shajib, A. J., Birrer, S., Treu, T., et al. 2019, *MNRAS*, 483, 5649

- Shajib, A. J., Glazebrook, K., Barone, T., et al. 2022, *LensingETC: a tool to optimize multi-filter imaging campaigns of galaxy-scale strong lensing systems*
- Shajib, A. J., Treu, T., Birrer, S., & Sonnenfeld, A. 2021, *MNRAS*, 503, 2380
- Shu, Y., Bolton, A. S., Moustakas, L. A., et al. 2016, *The Astrophysical Journal*, 820, 43
- Sluse, D., Chantry, V., Magain, P., Courbin, F., & Meylan, G. 2012, *A&A*, 538, A99
- Treu, T., Gavazzi, R., Gorecki, A., et al. 2009, *ApJ*, 690, 670
- Van de Vyvere, L., Gomer, M. R., Sluse, D., et al. 2022a, *Astronomy and Astrophysics*, 659, A127
- Van de Vyvere, L., Sluse, D., Gomer, M. R., & Mukherjee, S. 2022b, *Astronomy and Astrophysics*, 663, A179

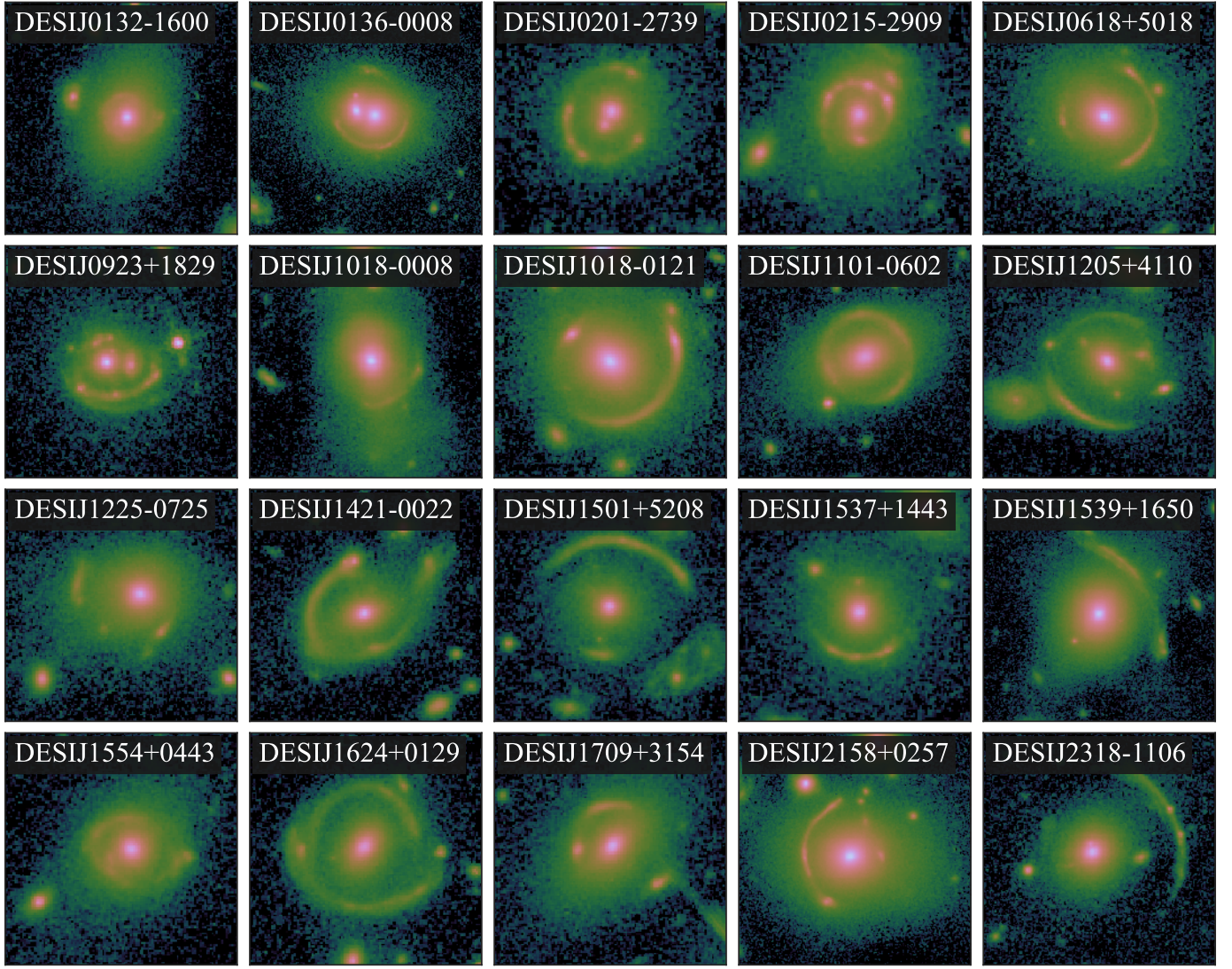


**Fig. 1.** Montage of all the lens systems.

**Table 1.** Lens model parameters:  $\theta_E$  is the Einstein radius,  $\gamma$  is the logarithmic slope of the mass profile,  $q_m$  is the mass axis ratio,  $\phi_m$  is the major axis position angle for mass,  $\gamma_{\text{shear}}$  is the residual shear magnitude and  $\phi_{\text{shear}}$  is the residual shear angle,  $R_{\text{eff}}$  is the effective radius of the light profile,  $q_L$  is the light axis ratio, and  $\phi_L$  is the major axis position angle for light. The point estimates are the medians of the 1D marginalized posteriors and the  $1\sigma$  uncertainties are obtained from the 16th and 84th percentiles.

System	$\theta_E$ (arcsec)	$\gamma$	$q_m$	$\phi_m$ (deg, N of E)	$\gamma_{\text{shear}}$	$\phi_{\text{shear}}$ (deg, N of E)	$R_{\text{eff}}$ (arcsec)	$q_L$	$\phi_L$ (deg, N of E)
--------	------------------------	----------	-------	---------------------------	-------------------------	--	------------------------------	-------	---------------------------



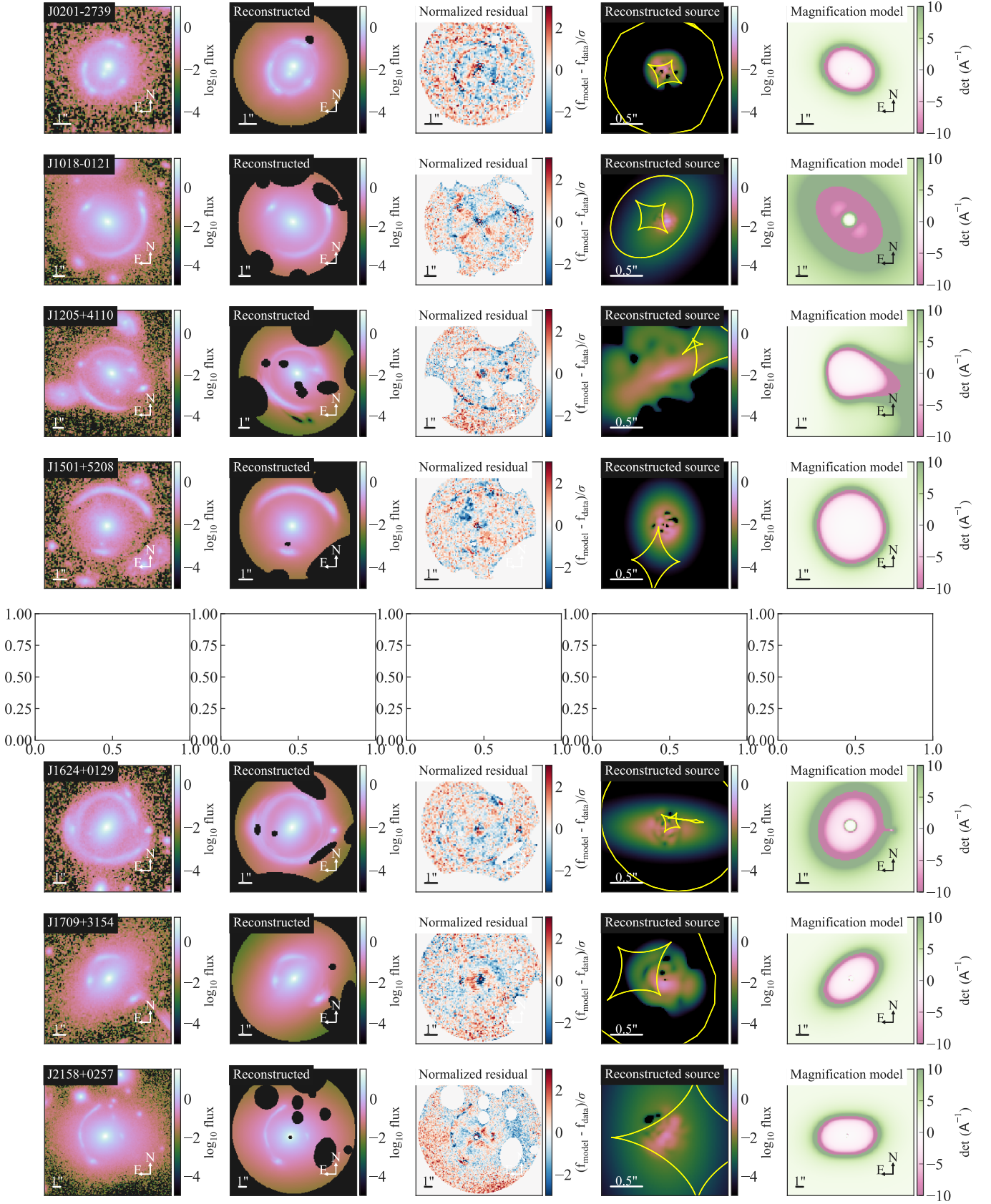


**Fig. 2.** Illustration of the lens models for the lens systems in our sample.